SUPPORTING INFORMATION

Is there a lower size limit for superconductivity?

Subhrangsu Sarkar,[1] Nilesh Kulkarni,[1] Ruta Kulkarni,[1] Krishnamohan Thekkepat,[2] Umesh Waghmare[2] and Pushan Ayyub[1]*

[1] Department of Condensed Matter Physics and Materials Science, Tata Institute of Fundamental Research, Mumbai 400005, India

[2] Theoretical Science Unit, Jawaharlal Nehru Centre for Advanced Scientific Research, Bangalore-560 064, India

Supporting Information

1. Synthesis of nanocrystalline α-Ta

2. Measurement techniques

3. Microstructure of representative nanocrystalline Ta samples.

4. Computational Methods: First-principles Calculations of Electronic DOS and Superconducting Parameters.

1. Synthesis of nanocrystalline α-Ta

Nanocrystalline thin films of phase-pure, body centred cubic (bcc) α-Ta were deposited by magnetron sputtering in an Ar atmosphere from a 99.9% pure 50mm-diameter Ta target. The base vacuum was ~10^{-7} mTorr and operating pressure of Ar was typically 5 mTorr. The substrates were Si <111> wafers previously coated with 400 nm thick SiO_2 layers using plasma-enhanced chemical vapor deposition (PECVD). During deposition, the substrates were placed 350 mm from the target and a stainless steel (SS304) mask was used to deposit the nanocrystalline thin films in the form of 300μm×1mm rectangular strips to facilitate subsequent four-probe measurements of electrical resistivity. The average crystallite size (d_{XRD}) was controlled by varying the sputtering conditions. Samples with larger d_{XRD} were deposited by dc sputtering, while rf sputtering was used to synthesise samples with smaller d_{XRD}. The average size was further controlled by varying the substrate temperature between 25°C and 800°C and the sputtering time between 10 and 30 min. In all, 12 nanocrystalline α-Ta thin film samples were prepared with mean crystallite size in the range: 2.4nm ≤ d_{XRD} ≤ 59nm and mean thickness between 40nm and 250 nm. In this range, the film thickness is not expected to affect the superconducting properties. XRD data showed that the Ta nanocrystals were oriented predominantly with their <110> axes normal to the film plane.

2. Measurement techniques

2.1. Powder x-ray diffraction (XRD) data were obtained using a Philips PANalytical's X'Pert Pro system. The line profile module X'Pert HighScore Plus 3.0e was employed to analyze the crystallographic phase and obtain the instrument-corrected coherently diffracting domain size (d_{XRD}) of the as-deposited nanocrystalline thin films of Ta.

2.2. The superconducting transition temperature (T_C) and critical magnetic field (H_C) were determined from four-probe electrical resistivity measurements on nano-Ta samples deposited in the form of 300μm×1mm rectangular strips down to 1.8 K using a Quantum design PPMS-14T (physical property measurement system). Samples with $T_C < 2.2$K were studied using a Quantum Design Dilution Refrigerator Option. Resistivity was measured using the Electrical Transport Option in the temperature range of 50mK to 4K, with a step size of 50mK in the vicinity of T_C.

2.3. The critical magnetic field, H_C, was determined from a set of resistance vs. magnetic field curves at different temperatures, by defining it as the magnetic field at which the resistance falls to $0.9R_N$, where R_N is the normal state resistance of the sample at that temperature. Since, not all of the measurements could be performed down to 50mK, we compare the values of upper critical magnetic field at a constant (though arbitrarily chosen) temperature, $T = 0.7 \times T_C$ and call this H_C.

3. Microstructure of representative nanocrystalline Ta samples.

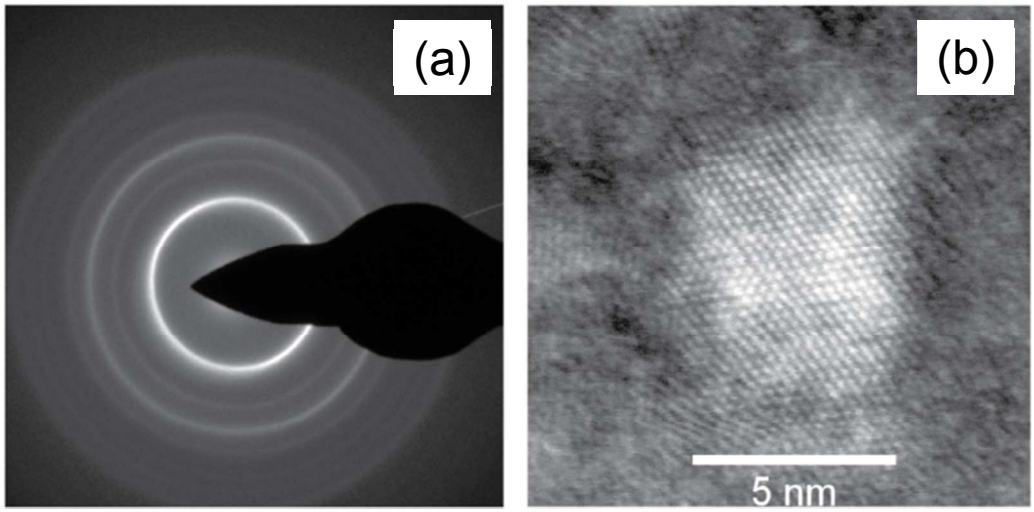

Figure S1. (a) Electron diffraction pattern of a sample with d_{XRD} = 7nm with bands at 2.41Å (d_{110}), 1.70Å (d_{200}) and 1.38Å (d_{211}) indicating a ≈3% expansion in '*a*'. (b) STEM image of a single Ta nanoparticle.

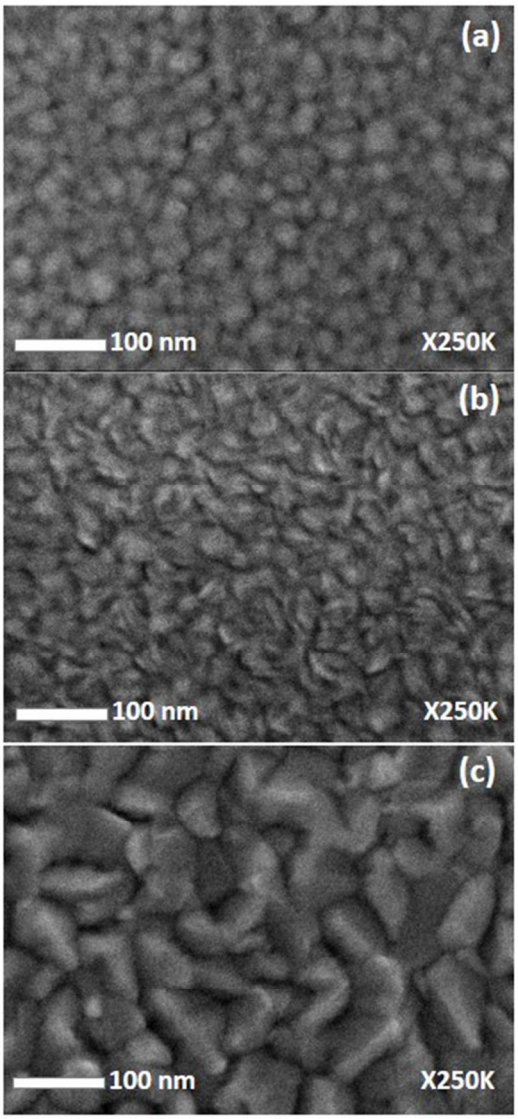

Figure S2. Scanning electron micrographs showing the surface microstructure of three representative nanocrystalline Ta samples with d_{XRD} = (a) 6.8 nm, (b) 10 nm, and (c) 59 nm. A Zeiss Ultra field-emission scanning electron microscope (FESEM) was used to study the surface morphology and thickness of the as-deposited samples after plasma cleaning. Note that each of the 'particles' seen in the SEM is an aggregate of a small number of crystallites.

4. Computational Methods: First-principles Calculations of Electronic DOS and Superconducting Parameters

Density functional theory (DFT) calculations on structures containing more than a few hundred atoms are extremely resource-intensive. In order to investigate the effect of the lattice expansion on the density of states (DOS) near the Fermi level, we performed the calculations on *bulk* Ta with the lattice constants being replaced by the experimentally observed set of values (for nano-Ta) with the cell geometry kept frozen during optimization. This is only a first approximation aimed at finding the nature of the changes in the DOS in Ta nanoparticles. One set of our first principles calculations were based on ATK-DFT module of Quantumwise atomistic toolkit[1,2] assuming generalized gradient approximation (GGA). We took account of the effect of spin-orbit coupling using the SOGGA exchange correlation. We used OMX pseudopotentials[3,4] with high (s3p2d2f1) basis set for our calculations to represent Kohn-Sham wavefunctions[5]. We used an energy cut-off value of 300 Hartree (8163.42 eV) for the basis set, and integration over the Brillouin zone was performed taking an uniform k-point mesh, whose value was optimized to be 30×30×30.

The effect of lattice strain on T_C was investigated using first principle density functional perturbation theory (DFPT) calculations[6]. The T_C was determined with the help of the PHonon package of Quantum Espresso[7] and following the suggestions of M. Wierzbowska *et al.*[8]. In the modified McMillan formula (see eqn. (1), main text), the electron-phonon mass enhancement parameter, λ, is expressed in terms of the phonon frequency, ω, and the average Eliashberg function, $\alpha^2F(\omega)$, as: $\lambda = 2\int[\alpha^2F(\omega)/\omega]\,d\omega$. For an electron of momentum $\boldsymbol{k}$ scattered into a band with momentum $\boldsymbol{k'}(=\boldsymbol{k}+\boldsymbol{q})$ due to an interaction with a phonon of energy ω belonging to a branch ν, the Eliashberg function is:

$$\alpha^2F_{\boldsymbol{kk'}}(\omega) = \frac{1}{N_F}\sum_{\nu}|g_{\boldsymbol{kk'}}|^2\delta(\omega-\omega_{\boldsymbol{kk'},\nu}) \qquad (1)$$

Here, the electron-phonon matrix element, $g_{\boldsymbol{kk'}}$, given by:

$$g_{\boldsymbol{kk'}}(\boldsymbol{p},i,j) = \left(\frac{\hbar}{2M\omega_{\boldsymbol{kk'}}}\right)^{\frac{1}{2}}\langle\psi_{i\boldsymbol{k}}|\frac{dV_{SCF}}{d\hat{u}_{\boldsymbol{kk'}}}|\psi_{j,\boldsymbol{p}+\boldsymbol{q}}\rangle \qquad (2),$$

while the phonon linewidth due to electron-phonon scattering, γ_{q_j}, is given by:

$$\gamma_{qv} = 2\pi\omega_{q,v}\sum_k \left|g_{k,k+q,v}\right|^2 \delta(\epsilon_k - E_F)\delta(\epsilon_{k+q} - \epsilon_k - \hbar\omega_{q,v}) \quad (3).$$

The average of the Eliashberg function can be expressed in terms of electron-phonon mass enhancement parameter as:

$$\alpha^2F(\omega) = \frac{1}{2}\sum_{q,v}\omega_{q,v}\lambda_{q,v}\delta(\omega - \omega_{q,v}), \text{ with: } \lambda_{q,v} = \frac{\gamma_{q,v}}{\pi N(E_F)\omega_{q,v}^2} \quad (4).$$

The density matrix of Ta in the relaxed and strained states was calculated by dividing the Brillouin zone into a dense 64×64×64 *k*-mesh. We used the Vanderbilt ultrasoft pseudopotential[9] and Perdew-Burke-Ernzerhof (PBE) exchange correlation energy functional[10] with plane wave basis set to represent Kohn-Sham wavefunctions[5]. We used energy cutoffs of 35 Ry and 320 Ry (which were their optimized values) to truncate the plane wave basis set used to represent the wave functions and charge densities respectively. The electronic density of states was calculated from the density matrix. To calculate the electron-phonon coupling coefficients, we used this density matrix data along with another set of density matrix data calculated on 16×16×16 *k*-mesh grid points with same $w_{cut\text{-}off}$ and $rho_{cut\text{-}off}$, which corresponds to calculation of phonons with a convergence threshold of 1×10^{-15}, for which, a *q*-mesh of grid size 4×4×4 was taken. The phonon calculation result was Fourier-transformed to get real space force constants and then interpolated to get the phonon dispersion, dynamical matrices and phonon band structure. Finally, these results were used to calculate λ, and T_C was computed using McMillan's formula.

[1]. Brandbyge, M.; Mozos, J.-L.; Ordejón, P.; Taylor, J.; Stokbro, K. *Phys. Rev. B* **2002,** *65*, 165401.

[2]. Soler, J. M.; Artacho, E.; D Gale, J. D.; García, A.; Junquera, J.; Ordejón, P.; Sanchez-Portal, D. *J. Phys. Condens. Matter* **2002**, 14, 2745–2779.

[3]. Ozaki, T.; *Phys. Rev. B* **2003**, *67*, 155108.

[4]. Ozaki T.; Kino, H. *Phys. Rev. B* **2004,** *69*, 195113.

[5]. Kohn, W.; Sham, L. J. *Phys. Rev.* **1965**, *140*, A1133--A1138.

[6]. Baroni, S.; de Gironcoli, S.; Corso, A. D.; Giannozzi, P. *Rev. Mod. Phys.* **2001**, *73*, 515–562.

[7]. Giannozzi, P.; Baroni, S.; Bonini, N.; Calendra, M.; Car, R.; Cavazzoni, C.; Ceresoli, D.; Chiarotti, G.L.; Cococcioni, M; Dabo, M. *J. Phys.: Condens. Matter* **2009**, *21***,** 395502.

[8]. Wierzbowska, M.; de Gironcoli, S.; Giannozzi, P. Preprint at https://arxiv.org/abs/cond-mat/0504077 v2 (2005).

[9]. Vanderbilt, D. *Phys. Rev. B* **1990**, *41*, 7892–7895.

[10]. Perdew, J. P.; Burke, K.; Ernzerhof, M. *Phys. Rev. Lett.* **1996**, *77*, 3865–3868.